ChemComm

Chemical Communications

rsc.li/chemcomm

ROYAL SOCIETY
OF **CHEMISTRY**
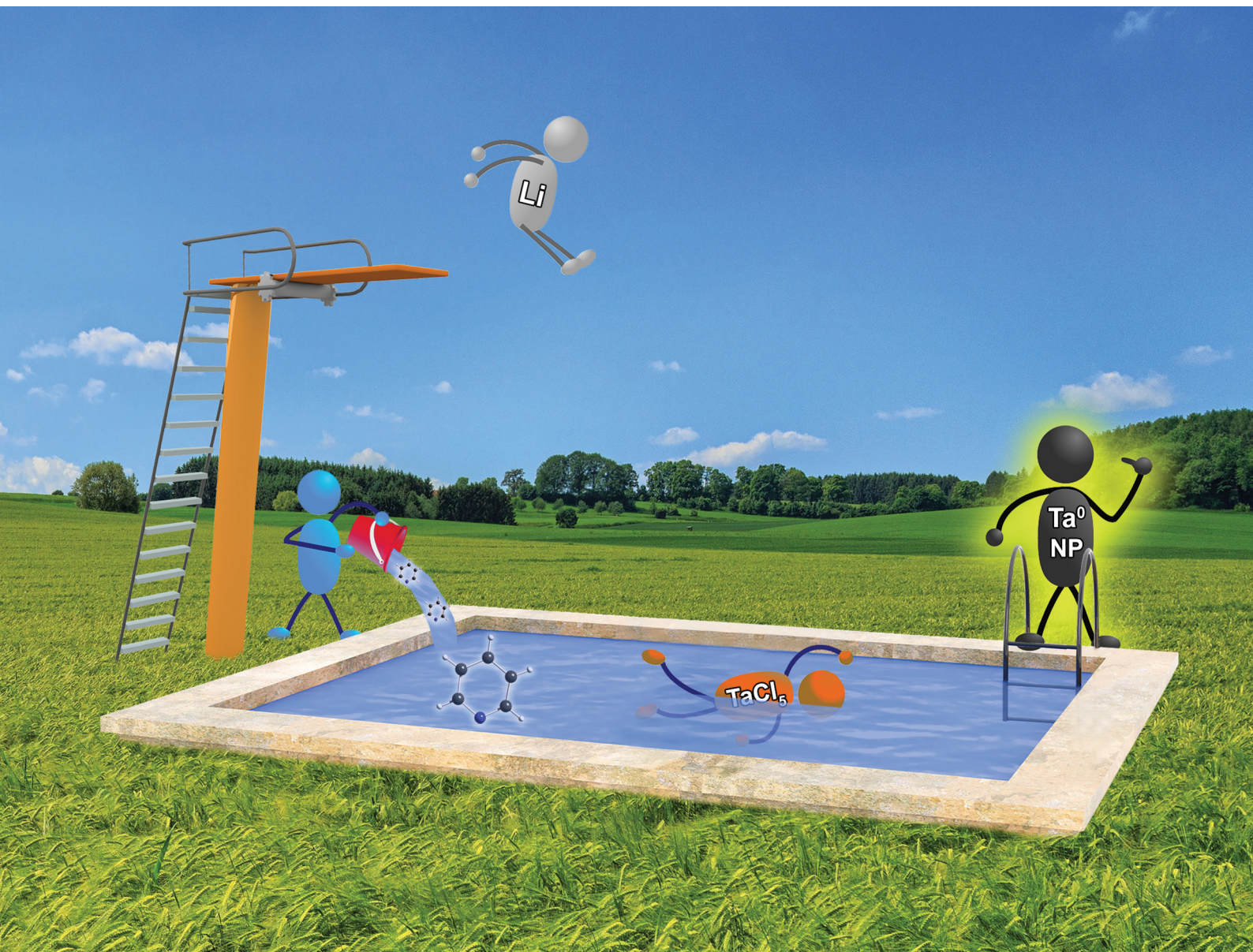
COMMUNICATION
Claus Feldmann *et al.*
Liquid-phase synthesis of highly oxophilic zerovalent
niobium and tantalum nanoparticles

Check for updates

Liquid-phase synthesis of highly oxophilic zerovalent niobium and tantalum nanoparticles†

Alexander Egeberg,[a] Lara-Pauline Faden,[a] Anna Zimina,[b] Jan-Dierk Grunwaldt, [b][bc] Dagmar Gerthsen[d] and Claus Feldmann [b] *[a]

Zerovalent niobium, Nb(0), and tantalum, Ta(0), nanoparticles are prepared *via* a one-pot, liquid-phase synthesis. For this, NbCl₅/TaCl₅ are dissolved in pyridine and reduced by lithium pyridinyl. Deep black suspensions of very small, highly uniform nanoparticles are obtained with average diameters of 2.1 ± 0.4 nm (Nb(0)) and 1.9 ± 0.4 nm (Ta(0)). Whereas suspensions are chemically and colloidally stable, powder samples are very reactive. TEM/HRTEM, XRD, FT-IR, and XANES are used for characterization.
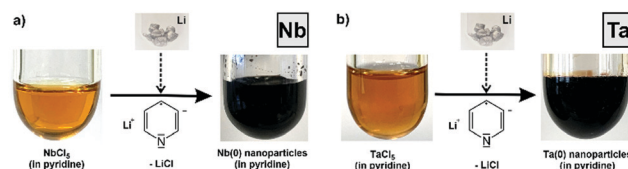
The hard metals niobium and tantalum are of general relevance in regard to hard materials and alloys.[1] Nowadays, both metals are also essential for capacitors in all kinds of electronic equipment such as mobile phones or computers.[2] In particular, the miniaturization of capacitors has significantly promoted the development of high-performance and low-weight devices.[1,2] Here, the availability of nanoparticles with uniform and small size is of general interest. Due to the distinct base character and the high oxophilicity of niobium and tantalum, however, the synthesis of high-quality nanoparticles (*i.e.*, narrow size distribution and high purity) is still a challenge.

To date, the options to prepare Nb(0) and Ta(0) nanoparticles are rare. Thus, the reduction of NbCl₅/TaCl₅ or Nb₂O₅/Ta₂O₅ by alkali metals or alkaline earth metals in molten salts (*e.g.*, LiCl–KCl–CaCl₂, CaCl₂) was reported.[3] Moreover, physical methods such as laser ablation, magnetron sputtering, physical vapor deposition, or hydrogen-arc plasma methods were suggested.[4] These methods were performed at elevated

temperatures (>300 °C) and typically result in broad size distributions in the range of 20-to-200 nm, often with significant oxide contaminations.[3,4] Liquid-phase strategies to obtain Nb(0) and Ta(0) nanoparticles were not reported until now. This situation can be ascribed to the experimental challenges, including the highly basic and oxophilic characters of niobium and tantalum. In the form of nanoparticles, both metals can be expected to be highly reactive due to the small size and the great number of surface atoms.

Aiming at nanoparticles of base metals, we have developed different synthesis strategies. These include microemulsions with liquid ammonia as the droplet phase, sodium-driven reduction in liquid ammonia, naphthalenide-driven reduction in ethers, or pyridinyl-driven reduction.[5] All these liquid phase methods have their specific pros and cons. Although we could successfully realize various base metal nanoparticles (*e.g.*, Re(0), Fe(0), Mn(0), Zn(0), and Ti(0)), the synthesis of Nb(0) and Ta(0) nanoparticles failed so far, which, again, can be ascribed to their distinct basic and oxophilic properties. Aiming at high-quality Nb(0) and Ta(0) nanoparticles, however, we recently have been successful by means of a one-pot, liquid-phase synthesis in pyridine (Fig. 1).

The synthesis of Nb(0) and Ta(0) nanoparticles was performed by using NbCl₅ and TaCl₅ as the starting materials. Both were dissolved in pyridine, resulting in an orange solution (Fig. 1). Thereafter, lithium was added to this solution with vigorous

[a] Institute for Inorganic Chemistry, Karlsruhe Institute of Technology (KIT), Engesserstrasse 15, Karlsruhe 76131, Germany. E-mail: claus.feldmann@kit.edu

[b] Institute of Catalysis Research and Technology, Karlsruhe Institute of Technology (KIT), Hermann-von-Helmholtz-Platz 1, Eggenstein-Leopoldshafen 76344, Germany

[c] Institute for Chemical Technology and Polymer Chemistry, Karlsruhe Institute of Technology (KIT), Engesserstraße 20, Karlsruhe 76131, Germany

[d] Laboratory for Electron Microscpy, Karlsruhe Institute of Technology (KIT), Engesserstrasse 7, Karlsruhe 76131, Germany

† Electronic supplementary information (ESI) available: Details related to the experimental equipment, reactivity, and evaluation of XANES spectra. See DOI: 10.1039/d1cc00681a

Fig. 1 Scheme illustrating the one-pot, liquid-phase synthesis of zerovalent niobium and tantalum nanoparticles: (a) reduction of NbCl₅ by Li[Py] in pyridine and (b) reduction of TaCl₅ by Li[Py] in pyridine with photos of dissolved NbCl₅/TaCl₅ and the resulting suspensions of Nb(0) and Ta(0) nanoparticles.

stirring. After a few minutes, the colour change from an orange solution to a deep black suspension indicates the reduction and formation of Nb(0) and Ta(0) nanoparticles (Fig. 1). Interestingly, we did not observe any significant effect on the particle size and suspension stability whether pre-dissolved lithium was added (*i.e.* Li[Py] in pyridine) or whether lithium was added as a solid (*i.e.* small pieces of the Li metal). This finding can be rationalized if the dissolution of the lithium metal in pyridine is significantly slower than the reduction of $NbCl_5$ and $TaCl_5$ by dissolved Li[Py]. In fact, this is in agreement with the experimental findings and was previously also observed for the formation of Fe(0) nanoparticles.[5d] The fast reduction was additionally confirmed by the very small size of the as-prepared Nb(0) and Ta(0) nanoparticles. Finally, the nanoparticles were purified by redispersion/centrifugation in/from pyridine and toluene. The Nb(0) and Ta(0) nanoparticles can be easily redispersed in pyridine or toluene to obtain colloidally and chemically stable suspensions (Fig. 1), or they can be dried in vacuum to obtain powder samples.‡ Suspensions and powder samples are chemically stable under inert conditions, whereas fast oxidation was observed, for instance, when in contact with air (ESI:† Fig. S1).

Particle size, particle shape, and size distribution of the as-prepared Nb(0) and Ta(0) nanoparticles were determined by electron microscopy (Fig. 2 and 3). Transmission electron microscopy (TEM) overview images and high-resolution (HR)TEM images show uniform, non-agglomerated nanoparticles with diameters of 1–3 nm (Fig. 2a, b and 3a, b). A statistical evaluation of >100 nanoparticles on the TEM
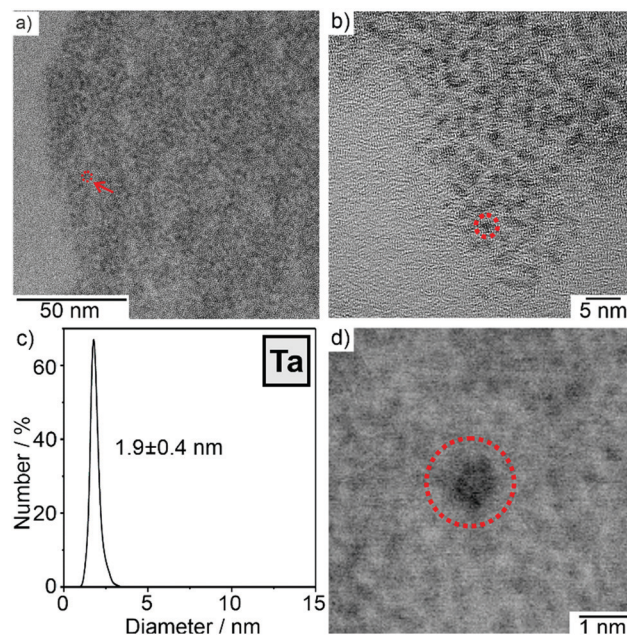

Fig. 3 Particle size, particle shape, and particle size distribution of the as-prepared Ta(0) nanoparticles: (a and b) overview TEM images at different levels of magnification, (c) size distribution based on the statistical evaluation of >100 nanoparticles on the TEM images, and (d) the HRTEM image of the selected nanoparticles. Single Ta(0) nanoparticles in (a, b and d) are indicated by red circles.
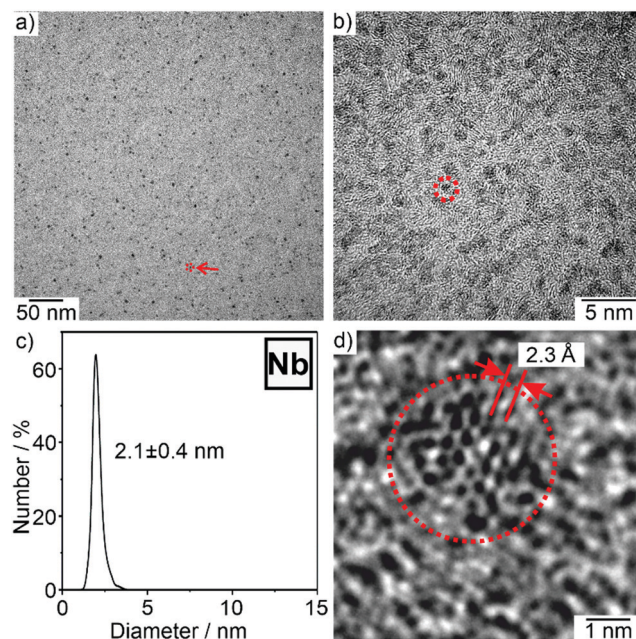

Fig. 2 Particle size, particle shape, and particle size distribution of the as-prepared Nb(0) nanoparticles: (a and b) overview TEM images at different levels of magnification, (c) size distribution based on the statistical evaluation of >100 nanoparticles on the TEM images, and (d) the HRTEM image of a nanoparticle with partial atomic order. Single Nb(0) nanoparticles in (a, b and d) are indicated by red circles.

images results in a narrow size distribution and mean particle sizes of 2.1 ± 0.4 nm for Nb(0) and 1.9 ± 0.4 nm for Ta(0) (Fig. 2c and 3c). In the case of Nb(0), the high-resolution (HR)TEM images indicate locally ordered atom configurations with parallel lattice fringes (Fig. 2d). The observed lattice fringe distance of 2.3 Å is well in agreement with cubic bulk-niobium (d_{110} with 2.3 Å).[6] The HRTEM images of the as-prepared Ta(0) nanoparticles do not show lattice fringes (Fig. 3d). The latter is to be expected for hard metals with high melting points ($T_{melt}(Nb(0)) = 2.477$ °C and $T_{melt}(Ta(0)) = 3.017$ °C).[7] In fact, it is more surprising to obtain crystalline niobium than to observe non-crystalline tantalum.

In addition to the first liquid-phase synthesis of Nb(0) and Ta(0) nanoparticles, Nb(0) and Ta(0) nanoparticles are realized with such a small size and narrow size distribution for the first time. The synthesis of very small nanoparticles with diameters of <4 nm is in accordance with the *LaMer-Dinegar* model.[8] Thus, the instantaneous reduction of the dissolved $NbCl_5/TaCl_5$ with [LiPy] and the insolubility of the zerovalent metals in pyridine result in a high supersaturation, which promotes a fast nucleation, and consequently, the formation of very small nanoparticles.

The presence and purity of the Nb(0) and Ta(0) nanoparticles was further validated by X-ray powder diffraction (XRD) analysis. Here, the as-prepared nanoparticles do not show any Bragg peaks, which can be ascribed to the small particle size and the low scattering power. After sintering of the powder samples at 900 to 1100 °C in an Ar/H_2 atmosphere, the Nb(0) and Ta(0) samples are crystalline and show the
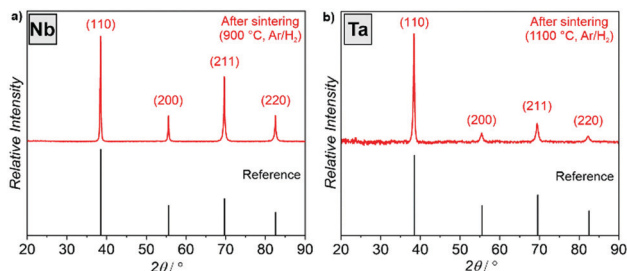
Fig. 4 X-ray powder diffraction analysis of Nb(0) and Ta(0) after sintering (900/1100 °C, Ar : H$_2$ = 95 : 5) with diffractograms of the bulk metals as references (Nb: ICDD-No. 00-035-0789 and Ta: ICDD-No. 00-004-0788).

characteristic Bragg peaks of bulk niobium and bulk tantalum (Fig. 4). Sintering in Ar/H$_2$ atmosphere was performed to avoid a reaction of the metal at elevated temperatures with pyridine adhered on the particle surface. Thus, sintering in Ar/H$_2$ resulted in the crystalline metals (Fig. 4), whereas sintering in Ar only led to the formation of carbides (ESI:† Fig. S2). Although the metals are of course not nanosized after sintering, the absence of impurity phases points to the purity of the as-prepared Nb(0) and Ta(0).

Fourier-transformed infrared spectroscopy (FT-IR) was used to evaluate the surface of the as-prepared Nb(0) and Ta(0) nanoparticles (Fig. 5). Due to the synthesis in pyridine the adhesion of solvent molecules on the nanoparticle surface is naturally to be expected. By comparison with pure pyridine as a reference, the observed low-intensity vibrations can be indeed related to pyridine. Moreover, elemental analysis (C/H/N analysis) results in 52.0/16.7 wt% C, 4.4/1.9 wt% H, 11.9/3.9 wt% N, and a residue of 31.7/77.5 wt%, which can be ascribed to Nb/Ta. When considering the nitrogen amount to originate from pyridine, the expected carbon and hydrogen amounts can be calculated as 51.0/16.7 and 4.3/1.4 wt%, respectively. Thus, the C/H/N amounts confirm pyridine to be adsorbed on the particle surfaces. The total amount of 68.3/22.5 wt% reflects the small particle size of the Nb/Ta nanoparticles and is in the expected range.

Although the nature and composition of the crystalline Nb(0) nanoparticles were already validated by HRTEM, we have additionally examined the oxidation state of the amorphous Ta(0) nanoparticles by X-ray absorption near edge structure (XANES) spectroscopy at the Ta-L$_3$ edge (Fig. 6). Beside the Ta(0)
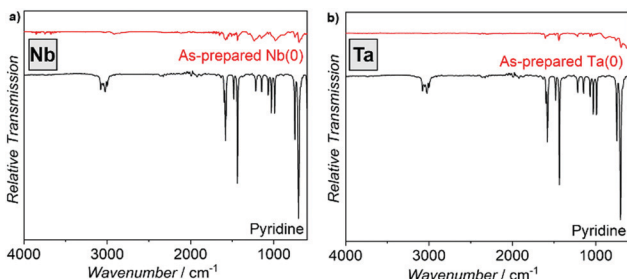

Fig. 5 FT-IR spectra of the as-prepared Nb(0) and Ta(0) nanoparticles with pure pyridine as a reference.
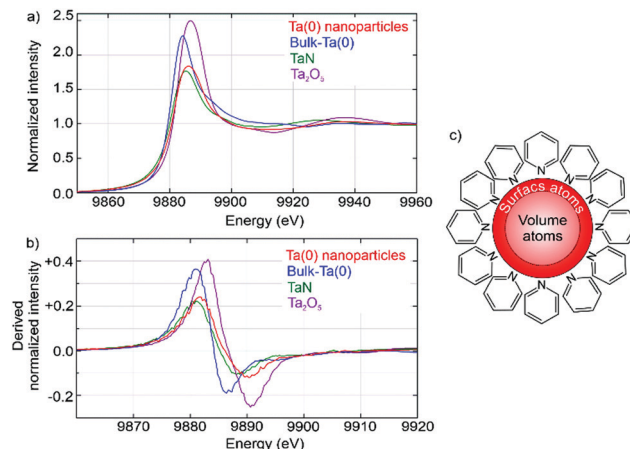

Fig. 6 XANES spectra of the as-prepared Ta(0) nanoparticles with bulk-Ta powder, TaN powder, and Ta$_2$O$_5$ powder as references: (a) Ta-L$_3$ spectra, (b) 1st derivative of XANES spectra in (a), and (c) scheme of Ta(0) nanoparticles with volume and surface atoms as well as pyridine-based surface functionalization.

nanoparticles, tantalum powder, TaN, and Ta$_2$O$_5$ were examined with tantalum in the formal oxidation states ±0, +III, and +V, respectively. The shape, intensity and energy position of all samples are very similar at first sight, but nevertheless exhibit certain differences (Fig. 6a). First of all, the as-prepared Ta(0) nanoparticles are clearly different from the Ta$_2$O$_5$ reference. The shape and energy position of the Ta(0) nanoparticles and Ta(0) and TaN powders, however, are very similar (Fig. 6a). Even the derived absorption does not show significant differences (Fig. 6b). To rationalize this observation, it needs to be noticed that volume atoms and surface atoms of the nanoparticles each show different behaviour. If the particle size is small enough, the surface atoms become more and more relevant. For the as-prepared Ta(0) nanoparticles with an average size of 1.9 ± 0.4 nm about 40% of the Ta atoms are located at the surface, where they are insufficiently coordinated in comparison to volume atoms, and where they show an additional interaction with pyridine adsorbed on the particle surface (Fig. 6c). Therefore, a significant contribution of the surface atoms, in addition to the volume atoms, is not a surprise. For metal clusters, moreover, the cluster size was reported to have a strong influence on the XANES spectra (e.g. argon-matrix-isolated metal clusters of Pr, Nd, and Sm).[9] Thus, the absorption edge of the clusters was observed to be shifted to higher energies in comparison to the bulk metal. Finally, the XANES spectra of Ta clusters supported on silica surfaces turned out to be very similar to the spectrum of the as-prepared Ta(0) nanoparticles (ESI:† Fig. S3).[10]

In conclusion, zerovalent niobium and tantalum nanoparticles were prepared via a one-pot, liquid-phase synthesis for the first time. Due to the highly basic character and the high oxophilicity of both metals, such liquid-phase synthesis is a challenge and requires handling under strict inert conditions for synthesis and all characterization. The liquid-phase synthesis of Nb(0) and Ta(0) nanoparticles was performed with NbCl$_5$/TaCl$_5$ as the starting materials that were reduced by

lithium pyridinyl in pyridine. The resulting deep black suspensions are colloidally and chemically very stable and contain very small, highly uniform nanoparticles with average diameters of 2.1 ± 0.4 nm for Nb(0) and 1.9 ± 0.4 nm for Ta(0). The reliable liquid-phase synthesis of Nb(0) and Ta(0) can become highly relevant in regard to high-quality hard materials, their properties and applications.

Conflicts of interest

There are no conflicts to declare.

Notes and references

‡ Experimental: All experiments and purification procedures were performed under an inert gas (argon), using the standard Schlenk techniques or glove boxes. This also includes all centrifugation and washing procedures. Moreover, the sample preparation and sample transfer for analytical characterization were strictly performed under inert conditions, e.g. by using specific transfer modules. Pyridine (ABCR, 99%) was refluxed for three days and freshly distilled over CaH_2. Toluene (Sigma-Aldrich, 99%) was purified by refluxing for three days and freshly distilled over sodium. Lithium (Riedel-de-Haën, 99%) was cut into pieces in an argon inert-gas atmosphere. Niobium(v)chloride (Sigma-Aldrich, 99%) and tantalum(v)chloride (Sigma-Aldrich, 99%) were used as received and handled in an argon inert-gas atmosphere.

Nb(0) nanoparticles: 150 mg of $NbCl_5$ was dissolved in 20 ml of pyridine. After addition of 19.1 mg of lithium, the orange solution started to turn to a black suspension after a few minutes with vigorous stirring, which indicates the formation of Nb(0) nanoparticles. This suspension was stirred for 24 hours at room temperature to complete the reaction. Thereafter, the deep black Nb(0) nanoparticles were washed three times by redispersion/centrifugation (25.000 U min^{-1}, 55.200 g) in/from pyridine and toluene. Finally, the Nb(0) nanoparticles can easily be redispersed in pyridine or dried in a vacuum to obtain powder samples. Optional sintering was performed under Ar/H$_2$-atmosphere (Ar : H$_2$ = 95 : 5).

Ta(0) nanoparticles: 200 mg of $TaCl_5$ was dissolved in 20 ml of pyridine. After addition of 19.1 mg of lithium, the orange solution started to turn to a black suspension after a few minutes with vigorous stirring. This suspension was stirred for 24 hours at room temperature to complete the reaction. Thereafter, the deep black Ta(0) nanoparticles were washed three times by redispersion/centrifugation (25.000 U min^{-1}, 55.200 g) in/from pyridine and toluene. Finally, the Ta(0) nanoparticles can easily be redispersed in pyridine or dried in a vacuum to obtain powder samples. Optional sintering was performed under Ar/H$_2$-atmosphere (Ar : H$_2$ = 95 : 5).

The XAS measurements were conducted at the Cat-Act-beamline at KIT's synchrotron radiation source.[11] The experiments at the Ta L$_3$-edge were conducted in fluorescence mode (see ESI†). The following reference compounds were used for XANES spectroscopy: Ta(0) powder (Sigma Aldrich, 99.99%), TaN (Alfa Aesar, 99.5%), and Ta_2O_5 (Fluka, ≥99.9%).

1 A. J. Padilla, Commodity Report 2020: Niobium & Tantalum, United States Geological Survey, Reston, 2020, pp. 114–115.
2 Y. Freeman, Tantalum and Niobium-Based Capacitors, Springer, Berlin, 2018.
3 (a) N. Wang, C. Du, J. Hou, Y. Zhang, K. Huang, S. Jiao and H. Zhu, Intermetallics, 2013, 43, 45–52; (b) N. Wang, K. Huang, J. Hou and H. Zhu, Rare Met., 2012, 31, 621–626; (c) M. Baba, Y. Ono and R. O. Suzuki, J. Phys. Chem. Solids, 2005, 66, 466–470.
4 (a) F. Azadi Kenari, S. Moniri, M. R. Hantehzadeh, D. Dorranian and M. Ghoranneviss, J. Mod. Opt., 2018, 65, 899–906; (b) S. Moniri, M. Ghoranneviss, M. R. Hantehzadeh and M. A. Asadabad, Soft Matter, 2017, 15, 153–162; (c) L. K. Brar, G. Singla, N. Kaur and O. P. Pandey, J. Therm. Anal. Calorim., 2015, 119, 175–182; (d) V. Singh, P. Grammatikopoulos, C. Cassidy, M. Benelmekki, M. Bohra, Z. Hawash, K. W. Baughman and M. Sowwan, J. Nanopart. Res., 2014, 16, 2373; (e) V. Singh, C. Cassidy, M. Bohra, A. Galea, Z. Hawash and M. Sowwan, Adv. Mater., 2013, 647, 732–737; (f) J. L. Barr, R. L. Axelbaum and M. E. Macias, J. Nanopart. Res., 2006, 8, 11–22; (g) Y. Wang, Z. Cui and Z. Zhang, Mater. Lett., 2004, 58, 3017–3020.
5 (a) F. Gyger, P. Bockstaller, D. Gerthsen and C. Feldmann, Angew. Chem., Int. Ed., 2013, 52, 12443–12447; (b) C. Schöttle, P. Bockstaller, D. Gerthsen and C. Feldmann, Chem. Commun., 2014, 50, 4547–4550; (c) C. Schöttle, P. Bockstaller, R. Popescu, D. Gerthsen and C. Feldmann, Angew. Chem., Int. Ed., 2015, 54, 9866–9870; (d) A. Egeberg, T. Block, O. Janka, D. Gerthsen, R. Pöttgen and C. Feldmann, Small, 2019, 15, e1902321.
6 N. Terao, Jpn. J. Appl. Phys., 1963, 2, 156–174.
7 J. Emsley, The Elements, Oxford University Press, Oxford, U. K., 1998.
8 V. K. La Mer and R. H. J. Dinegar, J. Am. Chem. Soc., 1950, 72, 4847–4854.
9 M. Lübcke, B. Sonntag, W. Niemann and P. Rabe, Phys. Rev. B: Condens. Matter Mater. Phys., 1986, 34, 5184–5190.
10 (a) J. Sun, M. Chi, R. J. Lobo-Lapidus, S. Mehraeen, N. D. Browning and B. C. Gates, Langmuir, 2009, 25, 10754–10763; (b) S. Nemana, J. Sun and B. C. Gates, J. Phys. Chem. C, 2008, 112, 7477–7485.
11 A. Zimina, K. Dardenne, M. A. Denecke, D. E. Doronkin, H. Huttel, H. Lichtenberg, S. Mangold, T. Pruessmann, J. Rothe, T. Spangenberg, R. Steininger, T. Vitova, H. Geckeis and J.-D. Grunwaldt, Rev. Sci. Instrum., 2017, 88, 113113.